Available online at www.sciencedirect.com
ScienceDirect
Tetrahedron
Tetrahedron 63 (2007) 10608–10614

Synthesis and properties of *N*,*N*,*N*′,*N*′-tetrasubstituted 1,3-bis(5-aminothien-2-yl)azulenes and their application as a hole-injecting material in organic light-emitting devices

Mitsunori Oda,[a,*] Nguyen Chung Thanh,[b] Masamichi Ikai,[c,*] Hisayoshi Fujikawa,[c] Keita Nakajima[b] and Shigeyasu Kuroda[b]

[a]*Department of Chemistry, Faculty of Science, Shinshu University, Asahi 3-1-1, Matsumoto, Nagano 390-8621, Japan*
[b]*Department of Applied Chemistry, Faculty of Engineering, University of Toyama, Gofuku 3190, Toyama 930-8555, Japan*
[c]*Toyota Central R&D Labs., Inc., Nagakute, Aichi 480-1192, Japan*

Received 11 June 2007; revised 6 August 2007; accepted 8 August 2007
Available online 10 August 2007

Abstract—Two title compounds, *N*,*N*,*N*′,*N*′-tetraphenyl-1,3-bis(5-aminothien-2-yl)azulene (**3a**) and 1,3-bis{5-(9-carbazolyl)thien-2-yl}azulene (**3b**), were synthesized from 1,3-di(2-thienyl)azulene (**4**) by a two-step sequence involving bromination and subsequent Pd-catalyzed amination. These compounds were characterized by spectroscopic analyses and the structure of **3a** was determined by X-ray crystallographic analysis. Their HOMO energy levels were estimated using their electrochemical oxidation potentials, and these compounds were used as a hole-injecting material in organic light-emitting devices. The device with **3a** showed greater durability than that with copper phthalocyanine.

1. Introduction

We previously reported the synthesis of *N*,*N*,*N*′,*N*′-tetrasubstituted 1,3-bis(4-aminophenyl)azulenes (**1a–c**) and their application as a hole-injecting (HI) material in organic light-emitting (OLE) devices.[1,2] These devices have recently received much attention because of their application in flat and thin panel displays, overcoming the drawbacks of contemporary electronic displays.[3,4] We also synthesized *N*,*N*,*N*′,*N*′-tetrasubstituted 1,3-bis(4-aminophenylethynyl)-azulenes (**2a–c**) for the same purpose but these compounds were found to be unstable for a fabrication process using vacuum deposition. We demonstrated that the diamines **1a–c** exhibit their prominent characteristics as a novel, durable, non-cyanine, and non-polyamine substance without color fade (Chart 1).

During the course of our continuing investigation of 1,3-diarylazulenes as an HI material, we have further studied structurally related compounds, **3**, which are formed by replacing the phenyl group of **1** with a thienyl group. We anticipated that the HOMO energy levels of **3**, similar to those of **1a–c**, could lie between indium-tin-oxide (ITO) work function and the levels of the commonly used hole-transporting (HT) materials, although the levels were expected to rise simply because of the relatively electron-donating nature of a thiophene ring compared with a phenyl ring. In this paper, we describe the synthesis and properties of **3** including the X-ray structural analysis of **3a**, and their application as an HI material in OLE devices.

2. Results and discussion

2.1. Synthesis of *N*,*N*,*N*′,*N*′-tetraphenyl-1,3-bis(5-aminothien-2-yl)azulene (3a) and 1,3-bis{5-(9-carbazolyl)thien-2-yl}azulene (3b)

We planned the synthesis of **3** by halogenation of 1,3-di(2-thienyl)azulene (**4**)[5–7] and subsequent Pd-catalyzed amination as reported for the synthesis of **1a–c**.[1,2] We previously described a four-step synthesis of **4** starting from a ketoester **5** via tetrahydroazulenone **6** (Scheme 1). This methodology is very useful for preparing azulenes with two different aryl groups at the 1- and 3-positions. However, we recently became aware that 1,3-diarylazulenes with the same aryl groups can be synthesized much more efficiently from 1,3-diiodoazulene (**7**), which is easily prepared from azulene by iodination with *N*-iodosuccinimide (NIS),[8] by Pd-catalyzed cross-coupling reactions.[2,6,7,9,10] In this work, we applied the latter method involving the cross-coupling

Keywords: Azulenes; Thiophenes; Amination; Organic light-emitting device; Hole-injecting material.
* Corresponding authors. Tel./fax: +81 263 37 3343 (M.O. for the molecular design, synthesis, and physical properties); tel.: +81 561 71 7183; fax: +81 561 63 6507 (M.I. for the EL application); e-mail addresses: mituoda@shinshu-u.ac.jp; m-ikai@mosk.tytlabs.co.jp

0040–4020/$ - see front matter © 2007 Elsevier Ltd. All rights reserved.
doi:10.1016/j.tet.2007.08.016

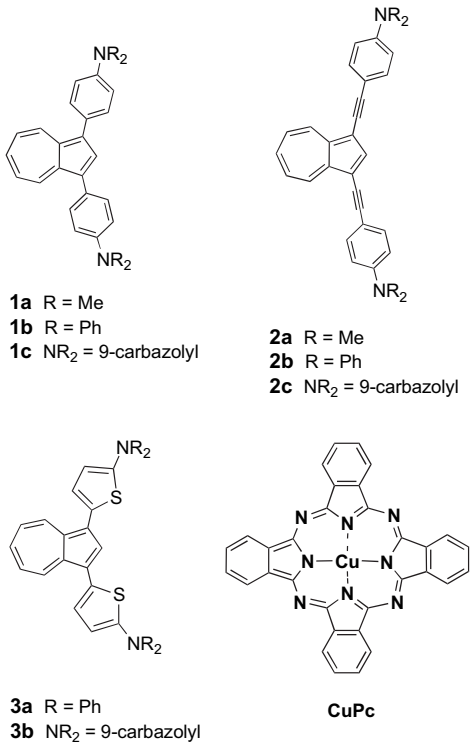

Chart 1.

reactions, instead of our previous method, for the preparation of **4**.

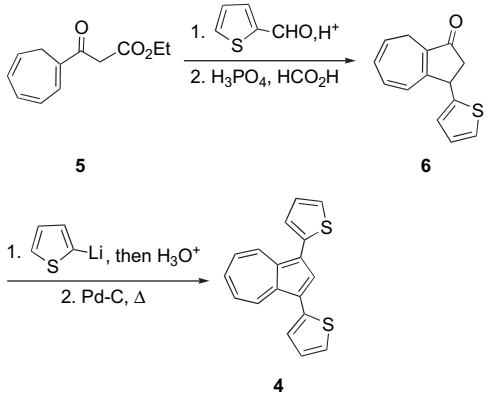

Scheme 1.

Although the Suzuki–Miyaura cross-coupling[11] of **7** with 2-thienylboronic acid was unsuccessful, the Stille cross-coupling[12] with 2-(tri-*n*-butylstannyl)thiophene (**8**) provided moderate to high yields of **4**. The results are summarized in Table 1. The use of tetrakis(triphenylphosphine)palladium as catalyst without additive gave a moderate yield of **4** (entry 1). The use of either CuI/CsF[13] or CuO[14] as an additive improved the yield (entries 2 and 3). In addition, **4** was obtained in good to high yields under the conditions of entries 4 and 6 with low loading of an expensive palladium catalyst.

The title compounds **3** were synthesized from **4** by bromination and subsequent Pd-catalyzed amination as shown in Scheme 2. While bromination of **4** with *N*-bromosuccinimide (NBS) yielded dibromide **9** in high yield, iodination

Table 1. The Stille cross-coupling of **7** with **8** under various conditions

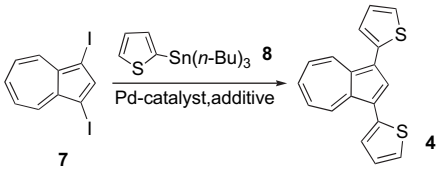

Entry	Pd catalyst, additive, solvent, temperature, time[a]	Yield of **4**[b] (%)
1	10%$Pd(PPh_3)_4$, DMF, 120 °C, 4 h	46
2	10%$Pd(PPh_3)_4$, 20%CuO, DMF, 120 °C, 4 h	90
3	7%$Pd(PPh_3)_4$, 300%CsF, 20%CuI, DMF, 40 °C, 3 h	98
4	2%$PdCl_2$, 8% (t-Bu)$_3$PHBF_4, 400%CsF, 8%CuI, 20%Cs_2CO_3, DMF, 40 °C, 2 h	94
5	1.5%Pd_2(dba)$_3$, 4% (t-Bu)$_3$PHBF_4, 200%CsF, 4%CuI, 10%Cs_2CO_3, DMF, 40 °C, 4 h	62
6	1.5%Pd_2(dba)$_3$, 12% (t-Bu)$_3$PHBF_4, 220%CsF, 220%Cs_2CO_3, dioxane, 100 °C, 4 h	83

[a] Two equivalents of **8** were used.
[b] Isolated yield after chromatographic purification.

with NIS gave only a trace amount of diiodide **10**. The yield of **10** was improved under conditions involving I_2 and $Hg(OAc)_2$, however only up to 37%. Because of the low yield of **10**, we used only **9** for the next amination step.[15] Under the Fu's conditions using (t-Bu)$_3$PHBF_4,[16] reactions of **9** with diphenylamine and carbazole gave the desired compounds, **3a** and **3b**, in 35 and 92% yields, respectively. We also attempted amination with volatile dimethylamine in a sealed glass tube. However, despite many efforts under various reaction conditions, **3c** has not been obtained yet.

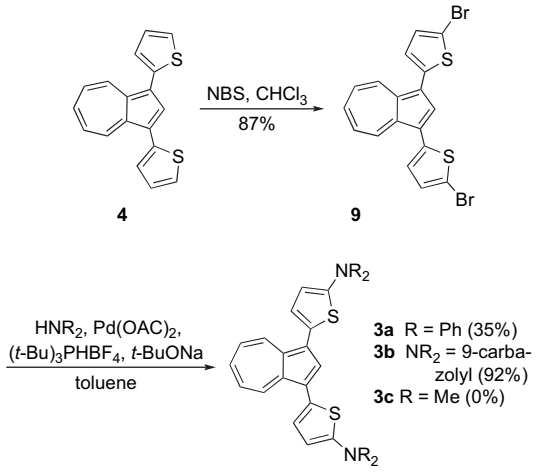

Scheme 2.

2.2. Physical properties and X-ray structural analysis of 3

The structures of **3a**,**b** were characterized by spectroscopic and combustion analyses. Signals in ^{1}H and ^{13}C NMR spectra were assigned by correlations based on their two-dimensional H–H COSY, HMQC and HMBC spectra, and NOE experiments; the results are shown in Figure 1. It should be noted that the assignment of the two thiophene protons, both of which appear as a doublet, was confirmed by the results of the NOE experiments shown in Figure 2.

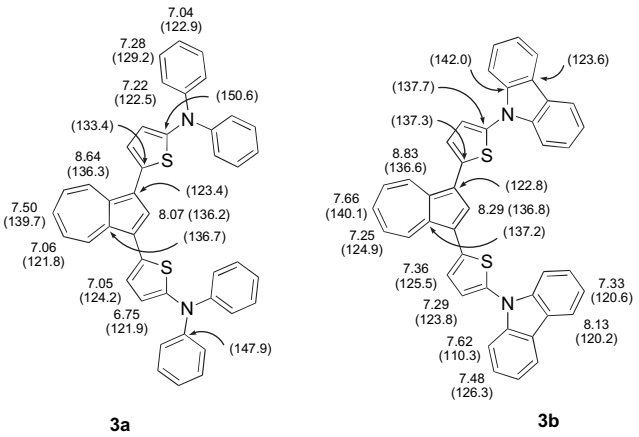

Figure 1. Assignment of ^{1}H and ^{13}C chemical shifts. Carbon shifts are in parentheses.

These compounds were isolated as green solids and their UV–vis spectra show two main, strong absorption bands at 280–310 and 330–390 nm and a weak broad band at 600–700 nm. The latter band in the visible range has a small extinction coefficient of 300–400, which is weaker than that of copper phthalocyanine (CuPc). These results are promising for overcoming the color fade observed with devices using CuPc. Electrochemical oxidation of **3a**,**b** was examined by cyclic voltammetry in dichloromethane containing 0.1 M tetra-*n*-butylammonium perchlorate. Each of the diamines **3a**,**b** showed two oxidation potentials (E^1_{ox} and E^2_{ox}) and the differences between the oxidation potentials are more than 0.33 V. The differences are large enough for the purpose of OLE applications.[17] The HOMO energy levels of these compounds were estimated as 5.15 eV for **3a** and 4.98 eV for **3b** based on the first oxidation potentials (Table 2). These levels are slightly less than that of CuPc (5.30 eV). The level of **3a** lies between those of HT materials, such as TPD (5.4–5.5 eV),[18] α-NPD (5.4 eV),[19] TPTE (5.3 eV),[20,21] and the work function of the ITO electrode (4.6–5.0 eV).[22] On the other hand, the level of **3b** is less than those of HT materials and is the same as the work function of the ITO electrode; i.e., the result concerning the HOMO energy level of **3b** is slightly different than expected (Chart 2).

The crystal structure of **3a** was determined by X-ray crystallographic analysis. Single crystals of **3a** were obtained

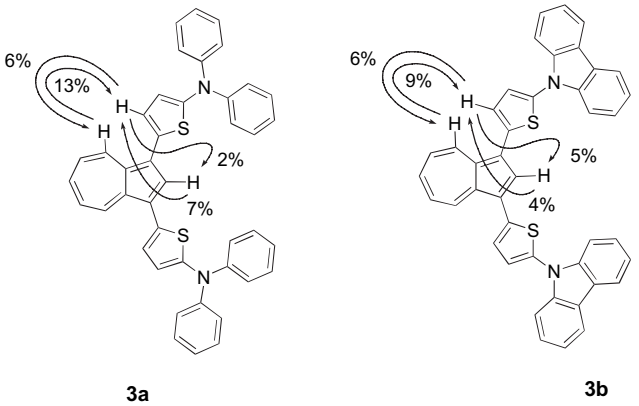

Figure 2. Results of NOE experiments of **3a**,**b**. Integral enhancements are noted relative to non-irradiated original integral area.

Table 2. Oxidation potentials and estimated HOMO energy levels of CuPc, and **3a**,**b**

Compounds	$E_{ox\ 1/2}$[a] (V vs Fc/Fc^+)		HOMO[b] (eV)
	E^1_{ox}	E^2_{ox}	
CuPc	0.51		5.30
3a	0.35	0.68	5.15
3b	0.18	0.64	4.98

[a] Corrected values from the E_{ox} (V vs SCE) by subtracting the E_{ox} value (0.48 V in dichloromethane, 0.50 V in *N*,*N*-dimethylformamide) of ferrocene in the same conditions. CuPc was measured in *N*,*N*-dimethylformamide and others were in dichloromethane.

[b] HOMO energy values were obtained from oxidation potentials (E^1_{ox}) against ferrocene and calculated by taking the HOMO energy value of ferrocene to be 4.8 eV with respect to zero energy level.

by recrystallization from a mixture of hexane and dichloromethane. ORTEP drawings and the crystal packing of **3a** are shown in Figures 3 and 4. There are two independent molecules of **3a**, **A** and **B**, in the unit cell with a slight difference in the bond lengths, angles, and conformations. Both structures are asymmetric. We recently reported the X-ray crystal structure of **4** in which both sulfur atoms are located at the side of the 2-position of the azulene ring and the two thienyl rings slant in different ways, up and down sides of the azulene plane.[23] This conformation of **4** is the most stable one predicted by DFT calculations. While the two thienyl rings in the structure of **A** connect with the azulene ring similarly to that seen in **4**, one of the sulfur atoms in the structure of **B** is located at the side of the 2-position of the azulene ring and

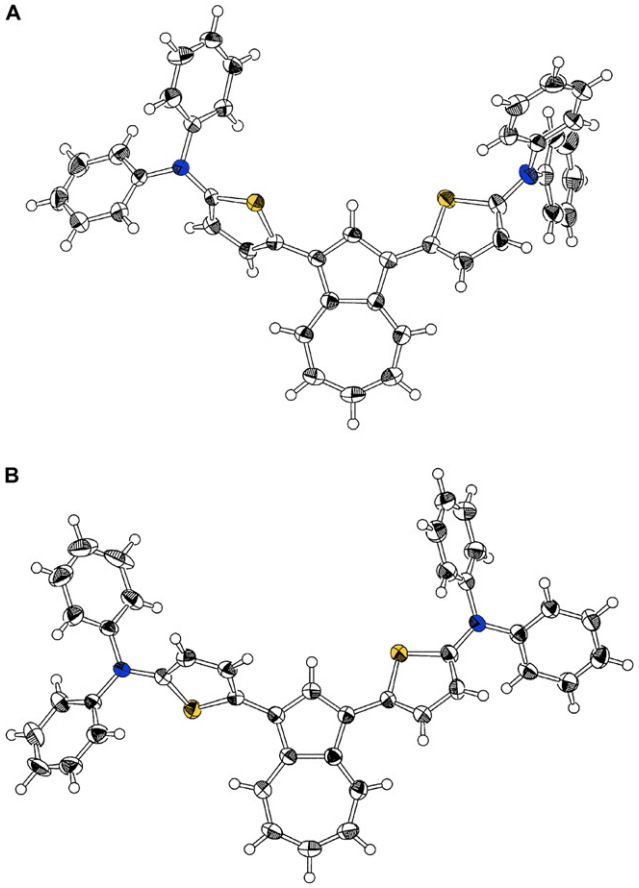

Figure 3. ORTEP drawings of two independent molecules of **3a** in the unit cell.

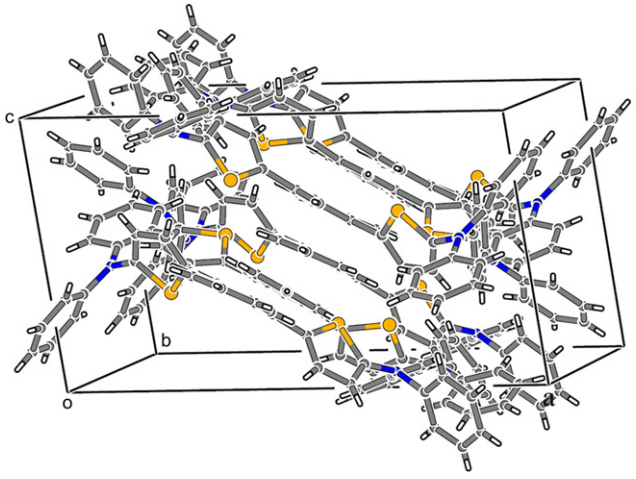

Figure 4. Crystal packing of **3a**.

the other at the side of the 4(8)-position. Energy differences between the possible conformers of **4** are not large,[24] and rotation around the C–C bond between the azulene and thienyl rings of **4** was predicted to be unrestricted based on DFT calculations.[22] Since the situation might be similar in **3a**, the packing may force the compound to take a suitable conformation to store the relatively large diphenylamino groups of **3a** in the cell. The azulene rings of the molecules **A** and **B** face each other, and the closest distance between the two seven-membered rings is 3.50 Å, which is slightly greater than twice the value of the van der Waals radius (1.7 Å) of carbon atom and therefore is not short enough to evidence π–π stacking between those rings.

2.3. Application of 3 as a hole-injecting material in OLE devices

An application of **3** in OLE devices investigated with the multilayered structure, which emits green light, is depicted in Figure 5. The initial characteristics and half-life at 11 mA cm^{-2} of current density are summarized in Table 3. Current density, voltage, and luminescence characteristics are shown in Figure 6. Although the luminance of the device with **3a** was slightly lower than that with CuPc, the driving voltage of the device was lower and its half-life was much longer than that with CuPc. Nevertheless, the half-life time of the device with **3a** is shorter than those of **1a–c** devices previously reported by us. On the other hand, while the luminance of the device with **3b** was greater than that with CuPc, the driving voltage of the device was higher and its half-life was much less than that of CuPc. The shortcomings of the latter device may be attributed to the HOMO energy level of **3b**, which does not lie appropriately between the ITO work function and the energy levels of the HT material used.

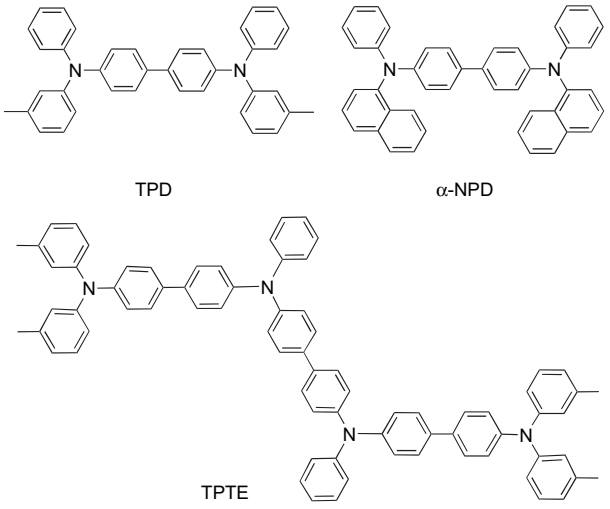

Chart 2. Structures of the HT materials.

Table 3. Initial characteristics and half-life time of the OLE devices with **3a**,**b** and CuPc as HI materials at 11 mA cm^{-2}

HIL materials	Initial luminance (cd cm^{-2})	Initial voltage (eV)	Half-life time (h)
3a	459	5.27	304
3b	556	7.47	50
CuPc	550	6.55	128

3. Summary

We have synthesized azulene derivatives, **3a** and **3b**, with aminothienyl groups substituted at the 1,3-positions from 1,3-di(2-thienyl)azulene (**4**) in two steps involving bromination and subsequent Pd-catalyzed amination. The starting material **4** was prepared from 1,3-diiodoazulene (**7**) in high yields by the Stille cross-coupling with 2-(tri-*n*-butylstannyl)thiophene (**8**). The structures of these compounds were fully characterized by spectroscopic analysis, and the crystal structure of **3a** was determined by X-ray crystallographic analysis. Their HOMO energy levels were estimated by electrochemical oxidation potentials to be higher compared with those of **1a–c**. While the level of **3a** lies between the ITO work function and the HOMO energy levels of commonly used HT materials, the level of **3b** is greater than the levels of the HT materials and is the same as the ITO work function. Application of these compounds as an HI material in OLE devices revealed that the device with **3a** was more durable than that with CuPc but was less durable than those with **1a–c**. From these results, it should be stressed that it is important to control the HOMO energy level of an HI material in OLE devices.

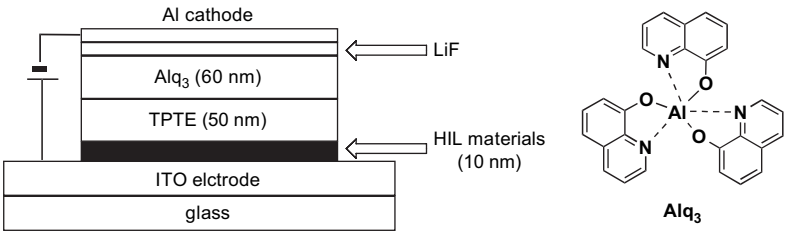

Figure 5. The OLE device architecture investigated.

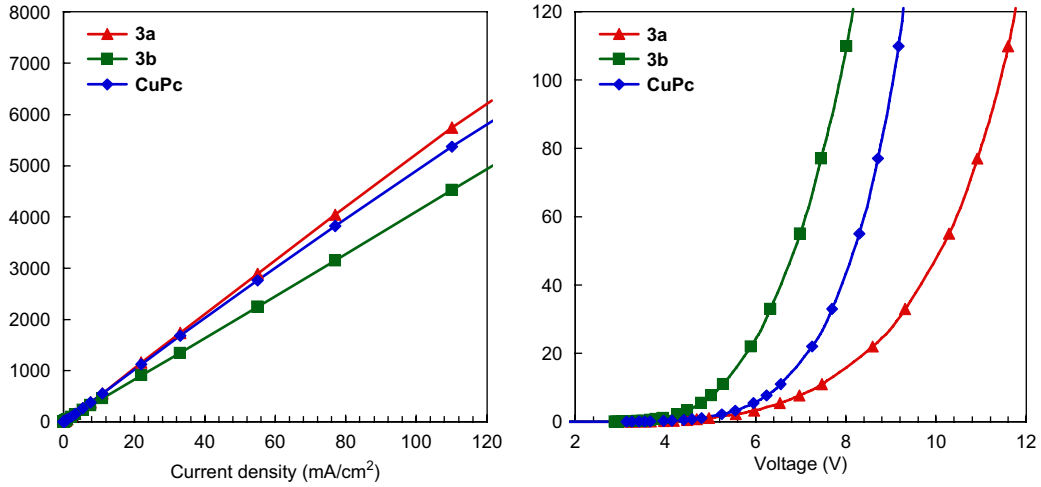

Figure 6. Current density, voltage, and luminescence characteristics of the OLE devices with **3a**,**b** and CuPc as HI materials; left (luminescence vs current density), right (current density vs voltage).

4. Experimental section

4.1. General

Melting points were measured on a Yanaco MP-3 and IR spectra were recorded on a Perkin–Elmer Spectrum RX I spectrometer. UV spectra were measured on a Shimadzu UV-1600 spectrometer. ^{1}H and ^{13}C NMR were recorded with tetramethylsilane as an internal standard on JEOL α400 and ECA600 NMR instruments. Mass spectra were measured on a JMS-700 mass spectrometer. Cyclic voltammograms were recorded on a Yanako P1100 instrument. Column chromatography was done with Wako activated alumina. Dioxane and *N*,*N*-dimethylformamide (DMF) were purified by distillation from calcium hydride under a nitrogen atmosphere. Diphenylamine and carbazole were purchased from Tokyo Kasei Ind. Co., cesium fluoride was purchased from Kanto Chem. Inc., tetrakis(triphenylphosphine)palladium, tris(dibenzylideneacetone)dipalladium, 2-(tri-*n*-butylstannyl)thiophene, and cesium carbonate from Aldrich Co., sodium *tert*-butoxide, NBS, iodine, tri-*tert*-butylphosphine, mercury acetate, palladium acetate, copper oxide, and copper iodide were from Wako Chem. Co. and all of them were used without purification.

4.2. Synthesis of 1,3-di(2-thienyl)azulene (4)

A mixture of 1,3-diiodoazulene (**7**, 1.00 g, 2.63 mmol), cesium fluoride (1.20 g, 7.80 mmol), and copper iodide (0.10 g, 0.52 mmol), tetrakis(triphenylphosphine)palladium (0.21 g, 0.184 mmol) and 2-(tri-*n*-butylstannyl)thiophene (1.7 ml, 5.40 mmol) in 20 ml of DMF were added and then this flask was evacuated and refilled with argon five times. The mixture was stirred at 40 °C for about 3 h until 1,3-diiodoazulene was almost consumed. Then the resulting reaction mixture was poured into water and extracted with ether (50 ml×3). The combined organic layer was washed with brine and dried over anhydrous $MgSO_4$. The solvent was removed under reduced pressure and the residue was purified by alumina column chromatography eluted with hexane to give 0.75 g (98%) of **4**[5] as dark green solids. Mp 131–133 °C (lit. 132–133 °C).

4.3. Synthesis of 1,3-bis(5-bromo-2-thienyl)azulene (9)

To a solution of **4** (300 mg, 0.96 mmol) in 10 ml of carbon tetrachloride at 0 °C was added 402 mg (2.25 mmol) of *N*-bromosuccinimide in several portions. After being stirred at 40 °C for 3 h, the reaction mixture was concentrated and the residue was purified by alumina column chromatography eluted with chloroform–hexane (3:7) to give 380 mg (87%) of **9** as dark green solids. Mp 136–138 °C. ^{1}H NMR ($CDCl_3$, 400 MHz) δ 8.62 (d, J=9.8 Hz, 2H), 8.00 (s, 1H), 7.62 (t, J=9.8 Hz, 1H), 7.19 (t, J=9.8 Hz, 2H), 7.12 (d, J=3.6 Hz, 2H), 7.00 (d, J=3.6 Hz, 2H) ppm; ^{13}C NMR ($CDCl_3$, 100 MHz) δ 140.2, 140.1, 137.1, 136.6, 136.4, 130.6, 125.4, 124.9, 122.2, 111.2 ppm; IR (KBr) ν_{max} 1571m, 1548w, 1388m, 960w, 868w, 844w, 800s, 741s cm^{-1}; UV–vis (CH_3OH) λ_{max} 241 (log ε=4.17), 303 (4.37), 323sh (4.30), 395 (3.76), 635 (2.29) nm; MS (70 eV) *m*/*z* (rel int): 452, 450, 448 (M^+, 60, 100, 37), 373 (9), 371 (7), 370 (10), 327 (8), 325 (9), 314 (13), 290 (9), 245 (15), 233 (8), 189 (19), 176 (9), 145 (8), 123 (8). Anal. Calcd for $C_{18}H_{10}Br_2S_2$: C, 48.02; H, 2.24. Found: C, 48.01; H, 2.34%.

4.4. Synthesis of 1,3-bis(5-iodo-2-thienyl)azulene (10)

To a solution of 1,3-(2-thienyl)azulene (**4**) (100 mg, 0.32 mmol), mercury acetate (102 mg, 0.32 mmol) and triethylamine (1.18 ml, 1.28 ml) in 10 ml of dichloromethane at 0 °C, 162 mg (0.64 mmol) of iodine was added. After being stirred at 0 °C for 1 h, the reaction mixture was extracted with chloroform (50 ml×3). The combined organic layer was washed with brine and a saturated aqueous solution of sodium thiosulfate, and was dried over anhydrous $MgSO_4$. The solvent was removed under reduced pressure and the residue was purified by alumina column chromatography eluted with chloroform to give 48 mg (37%) of **10** as dark green leaflets. Mp 139–141 °C. ^{1}H NMR ($CDCl_3$, 400 MHz) δ 8.62 (d, J=9.2 Hz, 2H), 8.01 (s, 1H), 7.62 (t, J=9.5 Hz, 1H), 7.31 (d, J=3.7 Hz, 2H), 7.20 (t, J=9.9 Hz, 2H), 6.94 (d, J=3.6 Hz, 2H) ppm; ^{13}C NMR ($CDCl_3$, 100 MHz) δ 144.7, 140.0, 137.7, 137.2, 136.7, 136.4, 126.7, 125.0, 122.1, 99.9 ppm; IR (KBr) ν_{max} 1563m, 1544w, 1403s, 938w, 851w, 790m, 739m cm^{-1};

UV–vis (CH_3OH) λ_{max} 209 (log ε=4.40), 243 (4.36), 305 (4.50), 416sh (3.90), 633 (2.37) nm; MS (70 eV) *m/z* (rel int): 546, 545, 544 (M^+, 51, 98, 100), 417 (29), 373 (59), 360 (62), 272 (38), 245 (34), 189 (61), 101 (24); Anal. Calcd for $C_{18}H_{10}I_2S_2$: C, 39.73; H, 1.85. Found: C, 40.04; H, 2.03%.

4.5. Synthesis of *N,N,N′,N′*-tetraphenyl-1,3-bis(5-aminothien-2-yl)azulene (3a)

To a suspension of 50 mg (0.11 mmol) of **9** and 40 mg (0.41 mmol) of sodium *tert*-butoxide in 5 ml of toluene were added 57 mg (0.33 mmol) of diphenylamine, 2.5 mg (0.011 mmol) of palladium acetate, and 6.4 mg (0.022 mmol) of $(t\text{-Bu})_3PHBF_4$. This flask was evacuated and refilled with argon five times. The mixture was heated at 110 °C for 48 h and then the resulting reaction mixture was poured into water and extracted with ether (30 ml×3). The combined organic layer was washed with brine and dried over anhydrous $MgSO_4$. The solvent was removed under reduced pressure and the residue was purified by alumina column chromatography eluted with chloroform–hexane (1:9) to give 64 mg (92%) of **3a** as dark green solids. Mp 132–134 °C. ^1H NMR ($CDCl_3$, 600 MHz) δ 8.64 (d, *J*=9.8 Hz, 2H), 8.07 (s, 1H), 7.50 (t, *J*=9.8 Hz, 1H), 7.28 (t, *J*=8.0 Hz, 8H), 7.22 (d, *J*=8.0 Hz, 8H), 7.05 (d, *J*=4.2 Hz, 2H), 7.06 (t, *J*=9.8 Hz, 2H), 7.04 (t, *J*=8.0 Hz, 4H), 6.75 (d, *J*=4.2 Hz, 2H) ppm; IR (KBr) ν_{max} 3033w, 1586s, 1544s, 1509m, 1491s, 1364m, 1273m, 1252m, 1074m, 1027m, 795m, 750s, 694s, 504m cm^{-1}; UV–vis (CH_2Cl_2) λ_{max} 300 (log ε=3.55), 337sh (3.44), 364 (3.46), 430sh (3.15), 660 (2.49) nm; MS (70 eV) *m/z* (rel int): 627 (M^++1, 50%), 626 (M^+, 100), 460 (9), 459 (28), 314 (6), 313 (12); Anal. Calcd for $C_{42}H_{30}N_2S_2$: C, 80.48; H, 4.82; N, 4.47%. Found: C, 80.50; H, 5.15; N, 4.37%.

4.6. Synthesis of 1,3-bis{5-(9-carbazolyl)thien-2-yl}azulene (3b)

To a solution of 50 mg (0.11 mmol) of **9** and 40 mg (0.41 mmol) of sodium *tert*-butoxide in 5 ml of toluene were added 55 mg (0.33 mmol) of carbazole, 2.5 mg (0.011 mmol) of palladium acetate, and 6.4 mg (0.022 mmol) of $(t\text{-Bu})_3PHBF_4$. This flask was evacuated and refilled with argon five times. The mixture was heated at 110 °C for 24 h and then the resulting reaction mixture was poured into water and extracted with ether (30 ml×3). The combined organic layer was washed with brine and dried over anhydrous $MgSO_4$. The solvent was removed under reduced pressure and the residue was purified by alumina column chromatography eluted with chloroform–hexane (1:9) to give 24 mg (35%) of **3b** as green solids. Mp 200–202 °C. ^1H NMR ($CDCl_3$, 600 MHz) δ 8.82 (d, *J*=9.9 Hz, 2H), 8.28 (s, 1H), 8.12 (d, *J*=8.1 Hz, 4H), 7.66 (t, *J*=9.9 Hz, 1H), 7.62 (d, *J*=8.1 Hz, 4H), 7.48 (t, *J*=8.1 Hz, 4H), 7.36 (d, *J*=3.6 Hz, 2H), 7.33 (t, *J*=8.1 Hz, 4H), 7.29 (d, *J*=3.6 Hz, 2H), 7.25 (t, *J*=9.9 Hz, 2H) ppm; IR (KBr) ν_{max} 3421w, 1599s, 1524w, 1509m, 1476m, 1447s, 1408m, 1332m, 1229s, 1163w, 838w, 810m, 741s, 720s, 635w cm^{-1}; UV–vis (CH_2Cl_2) λ_{max} 293 (log ε=3.76), 330sh (3.71), 340 (3.69), 410sh (3.61), 639 (2.62) nm; MS (70 eV) *m/z* (rel int): 623 (M^++1, 59%), 622 (M^+, 100), 540 (7), 539 (4), 537 (26), 459 (20), 457 (50), 312 (8), 311 (17); Anal. Calcd for $C_{42}H_{26}N_2S_2 \cdot H_2O$: C, 78.72; H, 4.40; N, 4.37%. Found: C, 78.85; H, 4.46; N, 4.33%.

5. Cyclic voltammetry

A standard three-electrode cell configuration was employed using a glassy carbon disk working electrode, a Pt wire auxiliary electrode, and an Ag wire as an Ag/Ag^+ quasi-reference electrode. The reference electrode was calibrated at the completion of each measurement on a saturated calomel electrode (SCE). Cyclic voltammetry was measured in a dichloromethane solution for **3a** and **3b** with tetrabutylammonium perchlorate as a supporting electrolyte and a scan rate of 0.1 V s^{-1} at 25 °C.

6. X-ray crystallographic analysis of *N,N,N′,N′*-tetraphenyl-1,3-bis(5-aminothien-2-yl)azulene (3a)

Prismatic crystals of **3a** were obtained by recrystallization from a mixture of hexane and dichloromethane. One of them having approximate dimensions of 0.40×0.30×0.40 mm was mounted on a glass fiber. All measurements were made on a Rigaku AFC7R diffractometer with graphite monochromated Mo Kα radiation and a rotating anode generator. Cell constants and an orientation matrix for data collection, obtained from a least-squares refinement using the setting angles of 20 carefully centered reflections in the range $25.41<2\theta<29.93°$, corresponded to a primitive triclinic cell with dimensions: a=17.378(7) Å, b=18.56(1) Å, c=10.456(4) Å, α=104.04(4)°, β=97.50(3)°, γ=83.57(4)°, V=3231(2) $Å^3$. For Z=4 and formula weight=626.83, the calculated density is 1.29 g cm^{-3}. Based on a statistical analysis of intensity distribution and the successful solution and refinement of the structure, the space group was uniquely determined to be $P\bar{1}(\#2)$. The data were collected at a temperature of –68±1 °C using the ω–2θ scan technique to a maximum 2θ value of 50.0°. Omega scans of several intense reflections, made prior to data collection, had an average width at half-height of 0.40° with a take-off angle of 6.0°. Scans of (1.42+0.30 tan θ)° were made at speeds of 16.0° min^{-1} (in omega). The weak reflections ($I<10.0\sigma(I)$) were rescanned (maximum of five scans) and the counts were accumulated to ensure good counting statistics. Stationary background counts were recorded on each side of the reflection. The ratio of peak counting time to background counting time was 2:1. The diameter of the incident beam collimator was 1.0 mm and the crystal to detector distance was 235 mm. The computer-controlled slits were set to 3.0 mm (horizontal) and 5.0 mm (vertical). Of the 10,019 reflections, which were collected, 9611 were unique (R_{int}=0.021). The intensities of three representative reflections were measured after every 150 reflections. No decay correction was applied. The linear absorption coefficient, μ, for Mo Kα radiation is 2.0 cm^{-1}. Azimuthal scans of several reflections indicated no need for an absorption correction. The structure was solved by direct methods and expanded using Fourier techniques. The non-hydrogen atoms were refined anisotropically. Hydrogen atoms were included but not refined. The final cycle of full-matrix least-squares refinement was based on 5612 observed reflections ($I>2.00\sigma(I)$) and 829 variable parameters and converged (largest parameter shift

was 0.00 times its esd) with unweighted and weighted agreement factors: R=0.042, Rw=0.052, and R_1=0.042 for $I>2.0\sigma(I)$ data. The standard deviation of an observation of unit weight was 1.23. The weighting scheme was based on counting statistics and included a factor (p=0.050) to downweight the intense reflections. Plots of $\Sigma w(|F_o|-|F_c|)^2$ versus $|F_o|$, reflection order in data collection, $\sin\theta/\lambda$ and various classes of indices showed no unusual trends. The maximum and minimum peaks on the final difference Fourier map corresponded to 0.22 and $-0.24\ e^-\ Å^{-3}$, respectively. Tables of fractional atomic coordinates, thermal parameters, bond lengths, and angles have been deposited at the Cambridge Crystallographic Data Center, 12 Union Road, Cambridge CB2 1EZ, United Kingdom (CCDC 645282).

7. OLE device fabrication

Organic layers were fabricated by high-vacuum (10^{-7}–10^{-6} Torr) thermal evaporation onto a glass substrate precoated with an ITO layer with a sheet resistance of 10 Ω per square. Prior to use, the ITO was degreased with solvents and cleaned in a UV-ozone chamber before loading into the evaporation system. A 10-nm thick CuPc, **3a**, or **3b** as the HI layer, a 50-nm thick TPTE as the HTL, a 60-nm thick Alq_3 as the light-emitting layer, a 0.5-nm thick LiF as the electron-injecting layer, and a 150-nm thick aluminum metal as a cathode were deposited on the substrate. Devices were encapsulated under nitrogen in a glass-to-glass epoxy sealed package.

Acknowledgements

We thank Dr. Ryuta Miyatake, University of Toyama, Toyama, for helping us to analyze the X-ray diffraction results of the compound **3a**. One of the authors (M.O.) is grateful to the Faculty of Science, Shinshu University, Matsumoto, for partial financial support.

References and notes

1. Oda, M.; Thanh, N. C.; Ikai, M.; Kajioka, T.; Fujikawa, H.; Taga, Y.; Ogawa, S.; Shimada, H.; Kuroda, S. *Chem. Lett.* **2005**, *34*, 754–755.
2. Thanh, N. C.; Ikai, M.; Kajioka, T.; Fujikawa, H.; Taga, Y.; Ogawa, S.; Zhang, T.; Shimada, H.; Miyahara, Y.; Kuroda, S.; Oda, M. *Tetrahedron* **2006**, *62*, 11227–11239.
3. Tang, C. W.; VanSlyke, S. A. *Appl. Phys. Lett.* **1987**, *51*, 913–915.
4. For reviews on organic electroluminescence, see books published recently: *Organic Electroluminescence*; Kafafi, Z. H., Ed.; CRC: Boca Raton, FL, 2005; *Organic Light Emitting Devices*; Müllen, K., Schrf, U., Eds.; Wiley-VCH: Weinheim, 2006.
5. Oda, M.; Kajioka, T.; Haramoto, K.; Miyatake, R.; Kuroda, S. *Synthesis* **1999**, 1349–1353.
6. Wang, F.; Han, M.-Y.; Mya, K. Y.; Wang, Y.; Lai, Y.-H. *J. Am. Chem. Soc.* **2005**, *127*, 10350–10355.
7. For other derivatives of **3**, see: Wang, F.; Lai, Y.-H. *Macromolecules* **2003**, *36*, 536–538; Wang, F.; Wang, F.; Lai, Y.-H.; Han, M.-Y. *Org. Lett.* **2003**, *5*, 4791–4794; Lai, Y.-H.; Han, M.-Y. *Macromolecules* **2004**, *37*, 3222–3230.
8. Hafner, K.; Patzelt, H.; Kaiser, H. *Liebigs Ann. Chem.* **1962**, *656*, 24–33.
9. Salman, H.; Abraham, Y.; Tal, S.; Meltzman, S.; Kapon, M.; Tessler, N.; Speiser, S.; Eichen, Y. *Eur. J. Org. Chem.* **2005**, 2207–2212.
10. Oda, M.; Kishi, S.; Thanh, N. C.; Kuroda, S. *Heterocycles* **2007**, *71*, 1413–1416.
11. For reviews on the Suzuki-Miyaura coupling reactions, see: Miyaura, N.; Suzuki, A. *Chem. Rev.* **1995**, *95*, 2457–2483; Suzuki, A. *J. Organomet. Chem.* **1999**, *576*, 147–168; Littke, A. F.; Fu, G. C. *Angew. Chem., Int. Ed.* **2002**, *41*, 4176–4211; Kotha, S.; Lahiri, K.; Kashinath, D. *Tetrahedron* **2002**, *58*, 9633–9695; Bellina, F.; Carpita, A.; Rossi, R. *Synthesis* **2004**, 2429–2440.
12. For reviews on the Stille coupling reactions, see: Echavarren, A. M. *Angew. Chem., Int. Ed.* **2005**, *44*, 3962–3965; Mitchell, T. N. *Metal-Catalyzed Cross-Coupling Reactions,* 2nd ed.; De Meijere, A., Diederich, F., Eds.; Wiley-VCH: Weinheim, 2004; 1, pp 125–161; Espinet, P.; Echavarren, A. M. *Angew. Chem., Int. Ed.* **2004**, *43*, 4704–4734; Spivey, A. C.; Gripton, C. J. G.; Hannah, J. P. *Curr. Org. Synth.* **2004**, *1*, 211–226.
13. Mee, S. P. H.; Lee, V.; Baldwin, J. E. *Angew. Chem., Int. Ed.* **2004**, *43*, 1132–1135.
14. Gronowitz, S.; Björk, P.; Malm, J.; Hörnfelt, A.-B. *J. Organomet. Chem.* **1993**, *460*, 127–129; Malm, J.; Björk, P.; Gronowitz, S.; Hörnfelt, A.-B. *Tetrahedron Lett.* **1994**, *35*, 3195–3196; Liu, C.-M.; Chen, B.-H.; Liu, W.-Y.; Wu, X.-L.; Ma, Y.-X. *J. Organomet. Chem.* **2000**, *598*, 348–352.
15. For reviews on the palladium-catalyzed aminations, see: Wolfe, J. P.; Wagaw, S.; Marcoux, J.-F.; Buchwald, S. L. *Acc. Chem. Res.* **1998**, *31*, 805–818; Hartwig, J. P. *Acc. Chem. Res.* **1998**, *31*, 852–860; Hartwig, J. P. *Angew. Chem., Int. Ed.* **1998**, *37*, 2046–2065.
16. Littke, A. F.; Dai, C.; Fu., G. C. *J. Am. Chem. Soc.* **2000**, *122*, 4020–4028; Netherton, M. R.; Fu, G. C. *Org. Lett.* **2001**, *3*, 4295–4298.
17. Plater, M. J.; Jackson, T. *Tetrahedron* **2003**, *59*, 4687–4692.
18. TPD is 4,4′-bis[*N*-(*m*-tolyl)-*N*-phenylamino]biphenyl Anderson, J. D.; Mcdonald, E. M.; Lee, P. A.; Anderson, M. L.; Ritchie, E. L.; Hall, H. K.; Hopkins, T.; Mash, E. A.; Wang, J.; Padias, A.; Thayumanavan, S.; Barlow, S.; Marder, S. R.; Jabbour, G. E.; Shaheen, S.; Kippelen, B.; Peyghambarian, N.; Wightman, R. M.; Armstrong, N. R. *J. Am. Chem. Soc.* **1998**, *120*, 9646–9655.
19. α-NPD is 4,4′-bis[*N*-(α-naphtyl)-*N*-phenylamino]biphenyl; the HOMO energy level was obtained from photoelectron measurements.
20. TPTE is 4,4′-bis{*N*-[*N*,*N*-di(*m*-tolyl)-4′-aminobiphenyl]-*N*-phenylamino}biphenyl; the HOMO energy level was obtained from photoelectron measurements.
21. Tanaka, H.; Tokito, S.; Taga, Y.; Okada, A. *Chem. Commun.* **1996**, 2175–2176.
22. Adachi, C.; Nagai, K.; Tamoto, N. *Appl. Phys. Lett.* **1995**, *66*, 2679–2681.
23. Ohta, A.; Thanh, N. C.; Terasawa, K.; Fijimori, K.; Kuroda, S.; Oda, M. *Tetrahedron Lett.* **2006**, *47*, 2815–2819.
24. The energy difference between the conformers corresponding to **A** and **B** types in **4** is predicted to be 0.466 kcal mol^{-1} by DFT calculations at B3LYP/6-31G(d) level of theory.